Vibrational Stark Effects of Nitriles I. Methods and Experimental Results

Steven S. Andrews and Steven G. Boxer*

Department of Chemistry, Stanford University, Stanford, CA 94305-5080

Received: June 21, 2000; In Final Form: October 19, 2000

Vibrational Stark effects, which are the effects of electric fields on vibrational spectra, were measured for the C−N stretch mode of several small nitriles. Samples included unconjugated and conjugated nitriles, and mono- and dinitriles. They were immobilized in frozen 2-methyl-tetrahydrofuran glass and analyzed in externally applied electric fields using an FTIR; details of the methodology are presented. Difference dipole moments, $\Delta\boldsymbol{\mu}$, equivalent to the linear Stark tuning rate, range from 0.01/f to 0.04/f Debye (0.2/f to 0.7/f cm^{-1}/(MV/cm)) for most samples, with aromatic compounds toward the high end and symmetric dinitriles toward the low end (the local field correction factor, f, is expected to be similar for all these samples). Most quadratic Stark effects are small and negative, while transition polarizabilities are positive and have a significant effect on Stark line shapes. For aromatic nitriles, transition dipoles and $\Delta\boldsymbol{\mu}$ values correlate with Hammett numbers. Symmetric dinitrile $\Delta\boldsymbol{\mu}$ values decrease monotonically with increasing conjugation of the connecting bridge, likely due to improved mechanical coupling and, to a lesser extent, an increased population of inversion symmetric conformations. $\Delta\boldsymbol{\mu}$ values are close to those expected from bond anharmonicity and ab initio predictions.

Introduction

When a weak electric field is applied across a molecule, both the molecular vibrational energy levels and the transition dipoles between the levels change slightly. These changes affect the infrared absorption spectrum of the sample, and are collectively called the vibrational Stark effect (VSE). VSE measurements yield information on the physics of molecular vibrations, including the anharmonicity of vibrational modes and the perturbation of chemical bonds by electric fields. VSE measurements can also be used to calibrate the sensitivity of a vibrational frequency to an electric field, called the Stark tuning rate, which allows an environmentally induced vibrational band shift to be used as a local probe of electrostatic fields.[1,2] Different vibrational modes have widely varying Stark effects, so a VSE spectrum can sometimes be used to identify a weak vibrational band of interest from a collection of overlapping background bands.[2]

Strong local electric fields are common in condensed matter systems, including the solvation of charged or dipolar molecules,[3] in ionic matrices, at electrode surfaces, across biological membranes,[4] and in the organized environment of proteins.[5,6] These local fields can be very large, typically lying in the range of 0.1 to 10 MV/cm. Vibrational band shifts have been studied in all these systems,[7−10] but in most cases neither the electric field nor the Stark tuning rate of the probe molecule was known accurately. We have recently shown that vibrational Stark spectroscopy is a useful tool for understanding vibrational band shifts for diatomic ligands bound to the heme iron in myoglobin.[1,2] We are also preparing to use vibrational Stark effects to calibrate the sensitivity of vibrational frequencies of C−N containing unnatural amino acids, such as cyano-phenylalanine and cyano-alanine, to determine fields in proteins. VSE will likely prove useful for understanding and predicting band shifts in a wide variety of other systems as well.

In this paper, a sensitive VSE measurement method is presented and used to analyze the C−N stretch mode of several small nitriles. Due to the paucity of work in vibrational Stark spectroscopy, we decided to survey a wide variety of nitriles including aromatic and aliphatic compounds, several homologous series of nitriles, and nitriles with varying degrees of symmetry. In the course of the work, it was found that many of the molecules studied, including several very simple ones, have multiple absorption bands in the nitrile frequency region. Where possible, the assignment of these bands is presented below, both to characterize the system being studied and because it influences the interpretation of the Stark data. Along with methods development, a primary objective of this work is to yield an understanding of the physical origins of vibrational Stark effects, which is introduced below and described more fully in a separate publication.[11]

The nitrile stretch mode was chosen for analysis for several reasons. The frequency is high enough to be well separated from most other vibrational modes and is in a spectral region that is relatively easy to detect, as it occurs near the maximum detectivity of an indium antimonide infrared detector. Bands are generally intense and narrow, properties which contribute to a strong Stark effect. A normal-mode analysis of organic nitriles shows that the nitrile stretch mode is highly localized to the nitrile bond,[12] which both simplifies the interpretation of VSE data and implies that changes to the rest of the molecule minimally perturb the nitrile normal mode. Finally, there is a great deal of experimental and theoretical literature on nitrile vibrations.[13−19]

Theory

A vibrational Stark analysis requires an absorption spectrum of the sample, $A(\bar{\nu})$, and a Stark difference spectrum, $\Delta A_\chi(\bar{\nu})$, which is the absorption in the presence of an external field, minus the absorption without the field. χ is the angle between the light polarization vector and the direction of the applied electric field, and can be varied from 90 to about 45 degrees using the experimental setup described in the next section. As

explained below, the absorption and Stark difference spectra are fit to give the Stark fit coefficients, from which are computed the Stark parameters of the sample.

Stark Parameters. For an absorption band, Stark effects are expected to yield a slight peak shift for each molecule in a sample, without any line shape change, where the shift is given by

$$\Delta\bar{\nu} = -\frac{1}{hc}\left(\Delta\boldsymbol{\mu}\cdot\mathbf{F} + \frac{1}{2}\mathbf{F}\cdot\Delta\boldsymbol{\alpha}\cdot\mathbf{F} + \cdots\right) \quad (1)$$

$\Delta\boldsymbol{\mu}$ and $\Delta\boldsymbol{\alpha}$ are called the difference dipole moment and the difference polarizability, respectively, referring to the differences between ground and excited states. These names are not entirely accurate for VSE due to field-induced bond changes,[20,11] but the variables are still useful and completely general. An electric field also affects the transition dipole moment, $\mathbf{M(F)}$, through the transition polarizability, $\mathbf{A}$, and the transition hyperpolarizability, $\mathbf{B}$

$$\mathbf{M(F)} = \mathbf{M} + \mathbf{A}\cdot\mathbf{F} + \mathbf{F}\cdot\mathbf{B}\cdot\mathbf{F} + \cdots \quad (2)$$

Again, the variables $\mathbf{A}$ and $\mathbf{B}$ are useful and general but the names are not entirely accurate for VSE.

As the samples studied in this work were immobilized in a frozen glass, the molecular orientations were isotropic (however, field-induced poling can be a problem and is discussed below). Integrating the peak shifts and extinction coefficient changes given in eqs 1 and 2 over all orientations, combined with the sample absorption spectrum, yields a computed Stark spectrum. This computed spectrum is a function of the two field-independent parameters, $\bar{\nu}$ and $\mathbf{M}$, and the four Stark parameters, $\Delta\boldsymbol{\mu}$, $\Delta\boldsymbol{\alpha}$, $\mathbf{A}$, and $\mathbf{B}$.

Stark Fit Coefficients. With the assumption that the absorption line shape is unaffected by the applied electric field, the computed Stark spectrum can be expressed as a sum of derivatives of the absorption spectrum[21]

$$\Delta A_x(\bar{\nu}) = |\mathbf{F}|^2 A_x A(\bar{\nu}) + \frac{|\mathbf{F}|^2}{15hc} B_\chi \bar{\nu} \frac{\partial}{\partial\bar{\nu}} \frac{A(\bar{\nu})}{\bar{\nu}} + \\ \frac{|\mathbf{F}|^2}{30h^2c^2} C_\chi \bar{\nu} \frac{\partial^2}{\partial\bar{\nu}^2} \frac{A(\bar{\nu})}{\bar{\nu}} \quad (3)$$

$\mathbf{F}$ is the electric field vector and A_χ, B_χ, and C_χ, which are called the zeroth, first, and second derivative coefficients, respectively, are found from eqs 1 and 2 to be

$$A_x = \frac{1}{3|\mathbf{M}|^2}\mathrm{Tr}(\mathbf{A}^T\mathbf{A}) + \frac{3\cos^2\chi - 1}{10|\mathbf{M}|^2}\left[(\mathrm{Tr}\mathbf{A})^2 + \mathrm{Tr}(\mathbf{A}^2) - \frac{2}{3}\mathrm{Tr}(\mathbf{A}^T\mathbf{A})\right] + \frac{2}{3|\mathbf{M}|^2}\sum_{i,j}M_i B_{ijj} + \\ \frac{3\cos^2\chi - 1}{5|\mathbf{M}|^2}\sum_{i,j}\left(M_i B_{jij} + M_i B_{jji} - \frac{2}{3}M_i B_{ijj}\right) \quad (4)$$

$$B_x = \frac{10}{|\mathbf{M}|^2}\mathbf{M}\cdot\mathbf{A}\cdot\Delta\boldsymbol{\mu} + \frac{3(3\cos^2\chi - 1)}{|\mathbf{M}|^2}\left(\Delta\boldsymbol{\mu}\cdot\mathbf{A}\cdot\mathbf{M} + \\ \mathbf{M}\cdot\Delta\boldsymbol{\mu}\,\mathrm{Tr}\mathbf{A} - \frac{2}{3}\mathbf{M}\cdot\mathbf{A}\cdot\Delta\boldsymbol{\mu}\right) + \frac{5}{2}\mathrm{Tr}\Delta\boldsymbol{\alpha} + \\ \frac{(3\cos^2\chi - 1)}{|\mathbf{M}|^2}\left(\frac{3}{2}\mathbf{M}\cdot\Delta\boldsymbol{\alpha}\cdot\mathbf{M} - \frac{1}{2}|\mathbf{M}|^2\mathrm{Tr}\Delta\boldsymbol{\alpha}\right) \quad (5)$$

$$C_\chi = 5|\Delta\boldsymbol{\mu}|^2 + (3\cos^2\chi - 1)(3\cos^2\zeta - 1)|\Delta\boldsymbol{\mu}|^2 \quad (6)$$

In eq 6, ζ is the angle between $\mathbf{M}$ and $\Delta\boldsymbol{\mu}$. There are also third derivative and higher order terms in the derivative expansion, but they are all proportional to the fourth or higher powers of the field, a dependence which is expected to be small and which was not seen in the data. The derivative coefficients were found from experimental data by fitting a measured Stark difference spectrum with a sum of the frequency-weighted derivatives of the absorption spectrum using software developed for this purpose. The fitting procedure is described below.

As the χ dependence in eqs 4−6 is restricted to a linear dependence on the term $3\cos^2\chi - 1$, only 6 scalar values of the 48 tensor components of the Stark parameters can be determined from Stark measurements, so a number of assumptions are needed to simplify the problem. The transition hyperpolarizability, $\mathbf{B}$, is assumed to be negligible, as it has been calculated to contribute at most a few percent to A_χ.[22] It is simplest to consider the molecular z axis to be parallel to the transition dipole moment, $\mathbf{M}$. In this system, $\Delta\alpha_{zz}$ and A_{zz} are parallel polarizability components, represented by $\Delta\alpha_{||}$ and $A_{||}$, and $\Delta\alpha_{xx}$, $\Delta\alpha_{yy}$, A_{xx}, and A_{yy} are the perpendicular polarizability components, represented by $\Delta\alpha_\perp$ and $A_\perp$, using the assumption that the perpendicular components are equal on the two axes. The off-diagonal components, representing polarizabilities perpendicular to an applied field, are assumed to be zero. With these simplifications, the six remaining Stark parameters are $|\Delta\boldsymbol{\mu}|$, $\Delta\alpha_{||}, A_{||}, \zeta, \Delta\alpha_\perp$, and $A_\perp$, which can be found from experimental data.

Further assumptions about the Stark parameters were made for data where the χ dependence of the Stark difference spectrum was not measured. Here, we assumed that a nitrile or dinitrile vibration behaves as a one-dimensional oscillator, with the result that ζ, $\Delta\alpha_\perp$, and $A_\perp$ are assumed to be zero. This assumption of a one-dimensional system is expected to be exact for nitriles with rotational symmetry about the nitrile bond (ignoring solvent induced asymmetry); it was also shown to be reasonably good for samples where the χ dependence was measured, described below.

Due to the bulk dielectric properties of the solvent as well as specific field-induced perturbations of the solvent near the sample molecules, the electric field at a sample molecule is greater than the average electric field (total applied voltage divided by electrode spacing). This difference is corrected for using the local field correction factor, f, which is estimated to be between 1.1 and 1.3,[23,24]

$$\mathbf{F}_{\text{local}} = f\,\mathbf{F}_{\text{external}} \quad (7)$$

Whereas the exact value of f is not known, it is expected to be the same constant for all experiments in this work, as well as for a great deal of other work, allowing for meaningful comparisons. Due to the lack of knowledge of this factor, results are reported in terms of factors of f.

Experimental

Samples were solutions of small aliphatic and aromatic nitriles in the glass forming solvent, 2-methyl-tetrahydrofuran (2-MeTHF). VSE sample concentrations ranged from 0.1 to 0.3 M, and no concentration dependent effects were observed throughout this range in either absorption or Stark spectra, indicating that nitrile dimers[18,25] did not form to a measurable extent. In support of this assertion, room temperature absorption spectra of several nitriles (butyronitrile, hydrogen cyanide,

Vibrational Stark Effects of Nitriles

J. Phys. Chem. A, Vol. 104, No. 51, 2000 **11855**

valeronitrile, and deuterated acetonitrile) also showed no concentration dependent effects for concentrations between 2.4 mM and 0.8 M. Low temperature extinction coefficients were measured by taking spectra of known sample concentrations with a setup that was essentially identical to that used for Stark measurements. The 2-MeTHF solvent and all nitriles, except for hydrogen cyanide, were purchased from Aldrich and used without further purification.

For the synthesis of hydrogen cyanide (HCN), equal volumes of 2-MeTHF and a 0.3 M aqueous solution of potassium cyanide were put in a vial, forming an organic layer on top of an aqueous layer. Dropwise addition of concentrated HCl formed the HCN product which partitioned into the organic layer, from which the sample was taken for spectroscopy. The partition coefficient (organic/aqueous) is 4.62, determined from room-temperature infrared peak intensities of HCN in the aqueous layer in contact with various volumes of 2-MeTHF. Using the partition coefficient, a known concentration of HCN was dissolved in the organic layer and used to determine the low-temperature extinction coefficient of HCN. It was shown with control experiments that no CN^- partitioned into the organic layer and that all measurable aqueous CN^- reacts to form HCN in the presence of excess acid. The room-temperature peaks analyzed here are aqueous CN^- at 2080 cm^{-1}, aqueous HCN at 2093 cm^{-1}, and organic HCN at 2079 cm^{-1}.

The infrared spectroscopy cell consisted of a pair of 13 mm diameter by 1 mm thick calcium fluoride windows (Janos Technology Inc.) with approximately 50 Å of nickel vacuum deposited on the surfaces facing the sample, a design which is similar to that used in previous work[26] and in electronic Stark spectroscopy.[24] A layer of nickel typically transmits 50 to 80% of the incident light throughout the infrared region, with the rest being either absorbed or reflected, and has a resistance of about 5 kΩ across the face of a window. The nickel electrodes were connected to a high voltage DC power supply (Trek Instruments Inc.), whose output voltage was synchronized to the FTIR scan timing, described below, with a home-built control unit. The windows were separated from each other by a pair of 28 micron thick Teflon spacers and held in place with a metal clamp. Using interference contour fringes, the windows were made parallel to within 1° to ensure both a uniform optical path length and a uniform field in the cell. The window separation in the center of the cell was measured to ± 0.05 micron after each experiment by taking a visible spectrum of the empty cell and measuring the frequency spacing between spectral interference fringes. After a sample was loaded into the cell by capillary uptake, it was rapidly frozen by immersing the cell in liquid nitrogen. This formed a transparent glass without observable cracks, crystallization, or other defects. The nitrogen immersion dewar is a custom built optical cryostat with several novel features designed to avoid bubbles and schlieren.[27]

Spectroscopy was carried out on a Bruker IFS 66V/S FTIR, with a nitrogen cooled indium antimonide detector and 0.5 cm^{-1} resolution. We first tried to record Stark spectra with the FTIR in step-scan mode, by locking into the second harmonic of a 200 hertz electric field applied to the sample. This is analogous to the standard method for visible and near-infrared Stark spectroscopy[24] and to a previous study of VSE[26] in which dispersive optics were used. Step-scan with lock-in detection has been used advantageously for measuring vibrational circular dichroism.[28] However, the noise reduction achieved by lock-in detection was more than offset by the noise gained by using step-scan mode. Better signal-to-noise was obtained using a DC electric field with the FTIR in its normal rapid-scan mode.[29]

Using this method, a single scan is made with the field turned off, then a scan with 2.5 kilovolts applied to the sample in one direction (about 0.9 MV/cm electric field), then another field-off scan, and finally a 2.5 kilovolt potential in the opposite direction. The alternating field pattern was chosen to avoid charge build-up in the sample and to prevent sample poling; both field-on scans gave identical spectra and were averaged together. This cycle was repeated at least 512 times, which is about 1 h, for each VSE measurement. At the end, the field-on and field-off interferograms were averaged and Fourier transformed; the ratio of their spectra were used to compute a Stark spectrum. The field-off spectrum, relative to background scans with the sample out of the light path, provided a good quality absorption spectrum with exactly the same conditions as the Stark spectrum. Sample molecules did not change their orientations due to the applied electric field in the immersion cryostat to any measurable extent, as determined by *(i)* the lack of differences between positive and negative field results after a constant positive field had been applied for 15 min or longer and *(ii)* the lack of a difference between sequential field-on scans, using a different electric field pattern.[30]

Data Analysis

Fits were made with at least one of three methods.[31] Where the absorption spectrum did not have overlapping bands, the numerical derivatives of the measured spectrum were used so as to eliminate errors due to naturally asymmetric line shapes or any consistent measurement error, such as light scatter or imperfect phase correction of the interferogram. This fitting method introduces the least error but cannot be used to determine separate Stark parameters for overlapping bands. For samples with overlapping bands, and for several samples with single bands in order the check the reliability of the method, the absorption spectra were fit first with a modified Voigt line shape for each peak. The form of a modified Voigt line shape is a linear combination of a Lorentzian and a Gaussian, where the Lorentzian and Gaussian are constrained to have the same peak positions and the same full width at half-maximum.[32] It is similar to a Voigt line shape, a convolution of a Lorentzian and Gaussian, and has similar versatility, but is easier to fit. The analytical derivatives of the separate peaks were then used to fit the VSE data, providing separate fit coefficients for each peak. The third method used a simultaneous fit of the absorption spectrum with modified Voigt line shapes, and of the Stark spectrum with the analytical derivatives of these line shapes. The sum of the two fit errors was minimized, where each least-squares error was weighted by the respective spectral rms noise, to use all the spectral information available for all the fit parameters. The simultaneous fitting method is less sensitive to noise in the absorption spectrum, but more sensitive to noise in the Stark data. Where multiple methods were carried out on the same set of spectra, fit results were identical, within statistical error.

To achieve a good signal-to-noise ratio, most data were obtained only at the experimental angle χ at 90°, where unpolarized light can be used and less of the infrared beam is clipped by the sides of the sample. These data were interpreted using the one-dimensional assumptions, described above. Fits to these data constrained A_χ values to be nonnegative, as negative values are impossible for a one-dimensional system and for a negligible transition hyperpolarizability (eq 4). This constraint was only required for data sets of poorer quality, suggesting that those A_χ values were dominated by noise and that the constraint is appropriate.

In some situations, strong interference fringes were observed at normal incidence due to reflections between the sample cell windows, which were reduced by rotating the sample away from the normal by up to 20° (still using unpolarized light). Those data were corrected to normal incidence, again with the assumption that the nitrile Stark effects follow one-dimensional behavior. The corrections are relatively insensitive to the assumptions for small rotation angles and unpolarized light.[33]

Despite rotating some samples, Stark spectra often showed a nonzero baseline, typically dominated by spectral interference fringes (about 130 cm^{-1} period), but also sometimes including a uniform offset or slope. To prevent the baseline from affecting the fit parameters, it was fit along with the rest of the Stark spectrum using a linear combination of a sine wave and a straight line. This did not interfere with the rest of the fitting because the baseline extended well beyond the nitrile peaks, and the functions used to fit the baseline yield very different curve shapes than the functions used to fit the VSE peaks.

The magnitudes of the transition dipoles were found from the area of the absorption band, expressed as an extinction coefficient spectrum, $\epsilon(\bar{\nu})$[34]

$$|\mathbf{M}| = \sqrt{\frac{3\epsilon_0 hc\ln 10}{2\pi^2 N_A \bar{\nu}} \int \epsilon(\bar{\nu})d\bar{\nu}} \qquad (8)$$

Several samples showed multiple peaks in the nitrile stretch region. For situations where the peaks were determined to be due to multiple vibrational modes, the peak areas were integrated separately using fits with modified Voigt line shapes (these samples include all dinitriles with multiple peaks and deuterated acetonitrile). On the other hand, where multiple peaks were determined to be due to either heterogeneity or Fermi resonance, the integration was carried out over all the peaks in order to include the entire sample and all the intensity of the nitrile mode (these samples include HCN and other aliphatic nitriles). Implicit in the latter method is the assumption that the transition dipole moments have the same magnitude for all nitrile stretches in a heterogeneous sample.

Results

Aliphatic Nitriles. The nitrile stretch mode of acetonitrile gives rise to an intense and narrow absorption band (Figure 1A). There is also a weak Fermi resonant peak 50 cm^{-1} to higher energy (not shown; peak maximum is at 2297.1 cm^{-1}, intensity is 6.90 M^{-1}cm^{-1}, fwhm is 20.1 cm^{-1}), which arises from resonance between the nitrile mode and the combination mode of the C−C stretch and the symmetric C−H bend.[8] To facilitate comparison with other spectra, Figure 1 and similar figures in this paper are scaled to show spectral extinction coefficients and to show Stark spectra for an applied field of 1 MV/cm (eq 3). The unscaled acetonitrile data, which are fairly typical, had a maximum absorption of 0.21 o.d., a minimum Stark absorption, relative to the baseline, of −4.4 × 10^{-4} o.d. using a 0.88 MV/cm electric field, and Stark rms noise levels of 5.2 × 10^{-6} o.d.

As seen in Figure 1C, the VSE spectrum is dominated by the second derivative of the absorption spectrum, but also shows significant zeroth and first derivative components (Table 1), all of which are highly reproducible. The χ angle dependence of the Stark spectrum was studied as well and is discussed below; however, it is ignored here and in Table 1, using the one-dimensional assumptions, to allow for a meaningful comparison with other nitriles where the χ dependence was not measured.
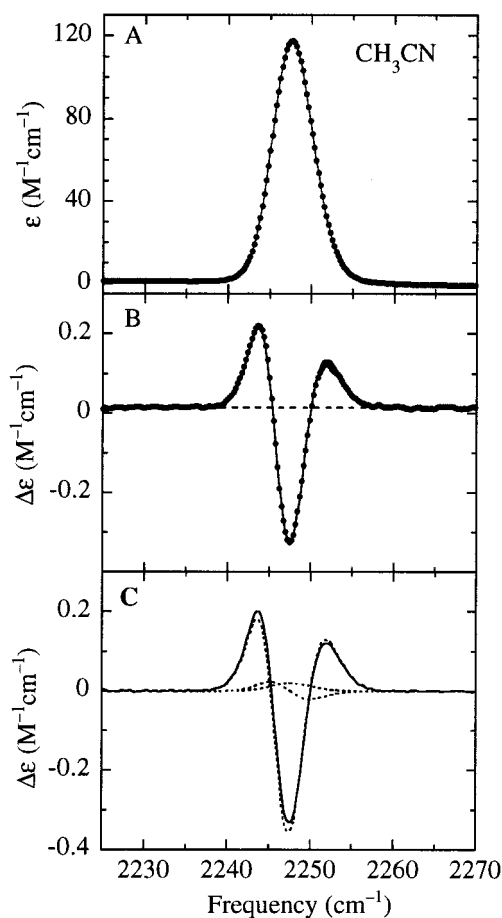
Figure 1. Spectra of acetonitrile. These and subsequent spectra are of samples dissolved in 2-MeTHF, at 74 K, and at normal incidence to the infrared beam. (A) Extinction coefficient spectrum of the nitrile stretch mode; the line is not a fit, but is simply shown to guide the eye. (B) Dots represent the Stark data, the solid line is the best fit to the Stark spectrum, using numerical derivatives of the data in panel A, and the dashed line is the Stark baseline. In this and subsequent figures, Stark spectra are scaled for a 1 MV/cm applied electric field. (C) The solid line is the fit from panel B, with the baseline subtracted, and the dashed lines are the zeroth, first, and second derivative contributions.

From the second and zeroth derivative contributions, respectively, $|\Delta\mu|$ is 0.0258 ± 0.0004 D/f and $A_{||}$ is 0.53 ± 0.03 Å^3/f, which imply a 0.43 cm^{-1} shift and a 6.1% increase of band intensity for molecules aligned parallel to a 1 MV/cm electric field (errors represent 1 standard deviation for 5 data sets). As $A_{||}$ is more than sufficient to account for the entire first derivative contribution, $\Delta\alpha_{||}$ is found to be slightly negative, with a value of −0.81 ± 0.07 Å^3/f^{2}, implying a band shift of 0.02 cm^{-1} to higher energy for molecules aligned parallel to a 1 MV/cm field. Due to the large width and low intensity of the resonant band, as well as its overlap with infrared absorption from liquid nitrogen in the immersion cryostat,[35,27] its Stark effect could not be measured reliably. However, its $|\Delta\mu|$ value appears to be between 0.01 and 0.05 D/f, putting it in the same range as the nitrile band Stark effect.

Deuterating acetonitrile lowers the C−H frequencies, which moves the Fermi resonant band well below the nitrile mode and moves the C−H stretch frequency to just below the nitrile mode (Figure 2 A, B). The two peaks were determined to have different Stark characteristics by the fact that derivatives of the entire absorption spectrum cannot be satisfactorily fit to the Stark spectrum. This required a separation of the peaks to allow independent fitting. However, the absorption spectrum cannot be fit with two modified Voigt line shapes due to the relatively

Vibrational Stark Effects of Nitriles

J. Phys. Chem. A, Vol. 104, No. 51, 2000 **11857**

TABLE 1: Vibrational Stark Effect Data for Unconjugated Aliphatic Nitriles

	absorption data				Stark data					
compound	$\bar{\nu}^a$ cm^{-1}	peak area M^{-1} cm^{-2}	|**M**| D	q e	A_χ 10^{20} m^2/V^2	B_χ 10^{40} Jm^2/V^2	C_χ 10^{63} J^{2}m^2/V^2	$\|\Delta\boldsymbol{\mu}\|^b$ D/f	$\Delta\alpha_{\parallel}^{b,c}$ Å^3/f^2	$A_{\parallel}^{b,c}$ Å^3/f
HCN L^d	2054.9	3989	0.134	0.79	15.8	2.23	28.89	0.0588	−4.93	3.55
HCN M^d	2064.7	3989	0.134	0.79	0	−2.92	20.12	0.0491	−1.76	0
HCN H^d	2072.4	3989	0.134	0.79	0	0.43	14.89	0.0422	0.26	0
acetonitrile^e	2247.5	830	0.058	0.36	1.8	0.22	5.56	0.0258	−0.81	0.53
propionitrile	2243.5	778	0.056	0.35	1.9	0.52	6.42	0.0277	−0.71	0.52
butyronitrile^e	2247.0	813	0.058	0.35	1.9	0.92	6.69	0.0283	−0.48	0.53
valeronitrile^e	2239.2	1024	0.065	0.40	0.5	0.87	5.95	0.0267	0.14	0.23
hexanenitrile^e	2243.2	793	0.057	0.35	0.5	−0.03	6.55	0.0280	−0.52	0.25
acetonitrile-d3	2255.5	974	0.063	0.37	2.1	−0.17	6.30	0.0275	−1.14	1.09
acetonitrile-d3 (C−D)^f	2234.5	904	0.061	0.39	7.2	1.77	14.16	0.0412	−1.89	0.60

^{a} Peak maximum. ^{b} Assumes one-dimensional behavior, i.e. $\zeta=0°$, and off-diagonal and perpendicular components of $\Delta\alpha$ and **A** are 0. ^{c} **B** is assumed to be 0. ^{d} Peak areas for HCN low (L), medium (M), and high (H) energy nitrile absorptions are combined. ^{e} Fermi resonant peaks are observed, and their areas are combined with the nitrile peak area. ^{f} C−D stretch mode of deuterated acetonitrile.
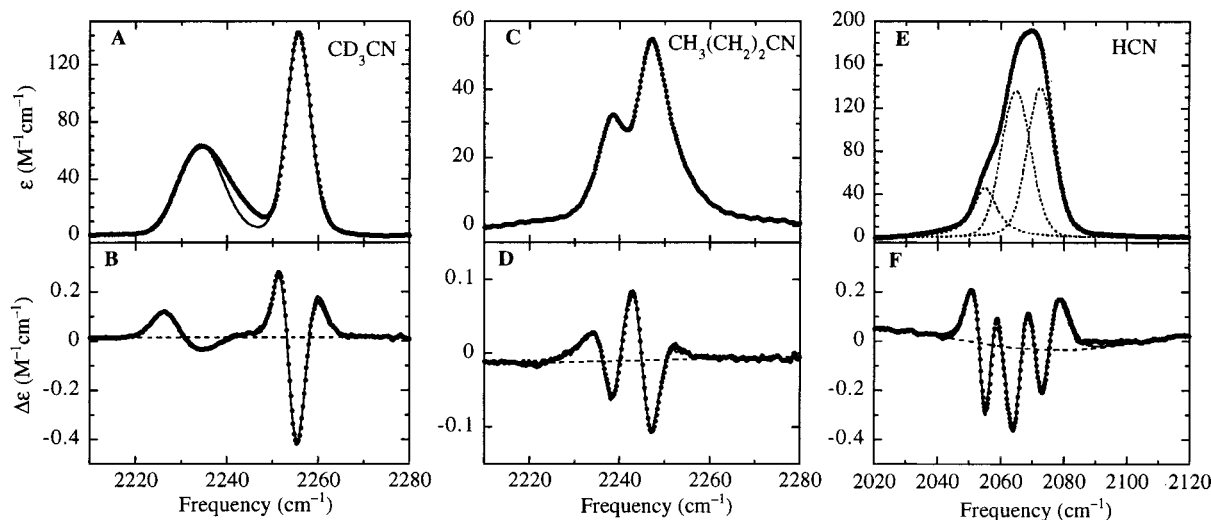
Figure 2. Spectra of CD$_3$CN, butyronitrile, and HCN. (A) Dots show the extinction coefficient spectrum for CD$_3$CN, showing a C−D stretch mode at 2235 cm^{-1} and the C−N stretch mode at 2256 cm^{-1}. The solid line is a sum of two modified Voigt line shapes, demonstrating the resonant absorption between the bands; these line shapes were used to separate the measured absorbance into two bands (see text). (B) Dots represent the CD$_3$CN Stark spectrum, the solid line shows the best fit to the Stark data, using different parameters for the two bands, and the dashed line shows the Stark baseline. (C, D) Extinction coefficient and Stark spectra for butyronitrile, where the two peaks are interpreted as being due to Fermi resonance. The line in panel C is shown to guide the eye, whereas the line in panel D is a fit to the Stark spectrum using numerical derivatives of the absorption spectrum, fit with a single set of coefficients. (E, F) Extinction coefficient and Stark spectra for HCN, where the three peaks are interpreted to result from heterogeneous hydrogen bonding to the solvent. Solid lines show fits that were made simultaneously to the two spectra, using modified Voigts for the extinction coefficient spectrum and their analytical derivatives for the Stark spectrum. Dashed lines in panel E show the three modified Voigt line shapes used to fit the peak, and the dashed line in panel F is the Stark baseline.

large absorption between the peaks, indicating the presence of nonlinear coupling between the C−N and C−D stretching modes.[36] A theory has not been developed yet for Stark effects of resonant modes, so an interpolation method was used to separate the peaks. It yielded a good fit to the data despite its lack of a physical basis. Two modified Voigt line shapes, called Fit$_L$ and Fit$_H$, were fit to the low and high energy peaks of the absorption spectrum, respectively, while ignoring the fit error of the region between the peaks (2237 to 2250 cm^{-1}). The ratios of the fits were used to separate the experimental spectrum, A, yielding separate spectra for the two peaks, A_L and A_H (these are all functions of $\bar{\nu}$)

$$A_L = \frac{A \cdot \text{Fit}_L}{\text{Fit}_L + \text{Fit}_H} \qquad A_H = \frac{A \cdot \text{Fit}_H}{\text{Fit}_L + \text{Fit}_H} \qquad (9)$$

As $A_L + A_H = A$, all the sample absorption is included without requiring the use of additional fitted peaks; the interpolation method also preserves the natural peak asymmetry. Derivatives of A_L and A_H were then fit to the Stark data (Figure 2B). The

good quality of the fit away from the region between the bands suggests that the fit parameters are likely to be representative of the isolated normal modes, and are thus comparable to parameters for other nitriles. Not surprisingly, the nitrile VSE parameters for deuterated acetonitrile (Table 1) are similar to those for protonated acetonitrile. For the C−D stretch mode, $|\Delta\boldsymbol{\mu}|$ is 0.0412 D/f, which is about 50% larger than the nitrile difference dipole.

A homologous series of aliphatic nitriles was studied, from hydrogen cyanide to hexanenitrile. With the exception of HCN (discussed below), the transition dipoles and difference dipoles are nearly identical across the series (Table 1). Other Stark parameters vary some, but with no clear trends and with less magnitude than the variation between aliphatic and other nitriles. The molecular polarizability changes by about a factor of 3 from acetonitrile to hexanenitrile,[37] suggesting that the molecular polarizability has a minimal influence on vibrational Stark effects for nitriles.

Lengthening the hydrocarbon chain to two units in propionitrile results in an absorption spectrum with a single peak and

no discernible Fermi resonance. However, on adding one, two, or three more CH_2 units to the hydrocarbon chain, giving butyronitrile, valeronitrile and hexanenitrile, respectively, the absorption spectra show a pair of peaks (Figure 2C shows butyronitrile). In all cases, the peaks fit well with a pair of modified Voigt line shapes, without any extra absorption between the peaks. Using the fits, the peak separations are 9.7, 13.0, and 13.0 cm^{-1} for the respective nitriles, while the ratios of the areas of the lower and higher frequency peaks are 0.22: 1, 1.38:1, and 0.006:1 (all at 74 K). Possible assignments for the multiple peaks include Fermi resonant interactions as seen for acetonitrile, heterogeneous sample conformations involving *anti* and *gauche* conformations, partial dimer formation in the sample, solvent heterogeneity, or a combination of these factors. These assignments do not affect the analysis of VSE data, although the interpretation varies considerably. From a variety of experiments, all of the possible assignments involving simple heterogeneity can be eliminated: (*i*) spectra are independent of sample concentration over a wide range of concentrations at both room temperature and at 74 K, indicating that dimer formation does not occur at the concentrations used; (*ii*) the relative areas of the peaks are different for different compounds, and none agree with the Boltzmann population calculations that the ratio of *gauche:anti* populations are expected to be about 0.07:1 in the frozen samples or 0.6:1 at room temperature;[38] (*iii*) the peak separations are much larger than those between homologous nitriles or than those calculated with AM1 methods for *gauche* and *anti* conformations (<1 cm^{-1}), also arguing against assignment based on conformational heterogeneity; (*iv*) room temperature spectra show multiple peaks and the solvent phase transition is not apparent in temperature dependent spectra, suggesting that solvation is not primarily responsible for the multiple peaks; and (*v*) room temperature spectra in toluene are very similar to those in 2-MeTHF, indicating again that specific solvation effects are not important. Thus, simple heterogeneity is unlikely, and the multiple peaks are almost certainly due, at least in part, to Fermi resonance. However, it remains surprising that Fermi resonance would yield significantly different spectra for each of the aliphatic nitriles studied. It is also surprising that the valeronitrile absorption spectrum shows a strong temperature dependence, whereas the other nitriles show a weak temperature dependence (data not shown).

As the intensity of the multiple peaks for butyronitrile, valeronitrile, and hexanenitrile is expected to arise from the nitrile mode (regardless of assignment), the entire band shapes were integrated to find the transition dipole moments. From VSE spectra (Figure 1D shows butyronitrile), it was found that the Stark parameters of the pairs of peaks are identical within measurement error, so they are reported in Table 1 with one value for each nitrile. Assuming the Fermi resonance assignment is correct, it is found that the Stark parameters of these Fermi resonant bands are identical to those of the parent bands, suggesting that VSE parameters represent the Stark effects of the source of the absorption intensity, rather than those of the forbidden mode. In contrast, recent work on the VSE of nitric oxide bound to the heme iron in myoglobin showed a case where Fermi resonance affects the Stark effect of the parent band.[2] In general, Stark effects of Fermi resonances are not well understood.

The simplest member of the aliphatic series, hydrogen cyanide, does not behave like the other aliphatic nitriles. Its absorption band is at lower energy, is broader, and is about 4 times more intense (Figure 2E, F). The simplest fit that can be made to the absorption and Stark spectra requires three
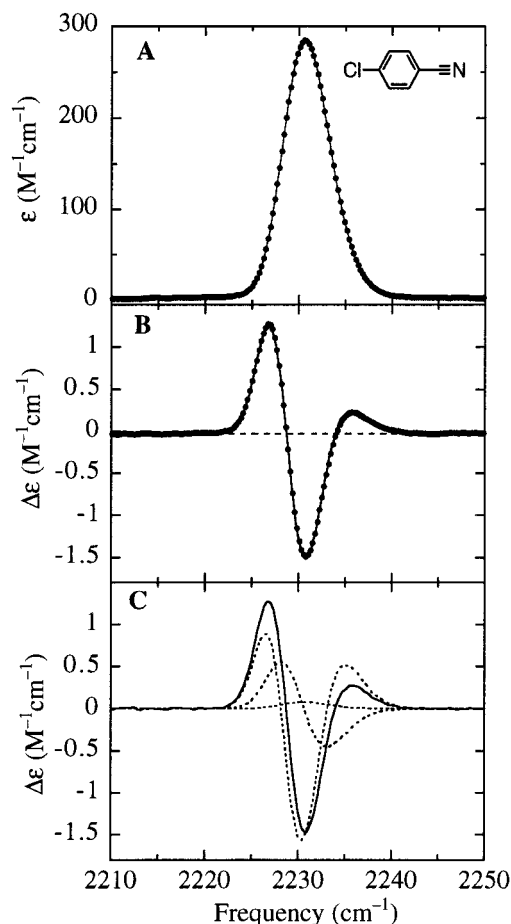
Figure 3. Spectra of 4-chloro-benzonitrile. (A) Extinction coefficient spectrum, where the line is shown to guide the eye. (B) Dots represent the Stark spectrum, the solid line is the best fit to the Stark spectrum using numerical derivatives from panel A, and the dashed line is the Stark baseline. (C) The solid line is the fit from panel B with the baseline subtracted, and the dashed lines are the zeroth, first, and second derivative contributions.

overlapping modified Voigt line shapes, characterized by different Stark parameters. Due to the simplicity of HCN, there are no resonant modes or alternate conformations; consequently, the three peaks most likely represent heterogeneous hydrogen bonding from the sample to the 2-MeTHF solvent. This interaction, which cannot occur for the other samples, would be expected to significantly affect the nitrile bond. In agreement with this assignment, the spectrum of HCN exhibits a single broad peak when it is dissolved in 2-MeTHF at room temperature, and a single sharp peak when in a toluene glass at low temperature. The transition dipoles were considered to be the same for the three heterogeneous peaks, despite the fact that this is likely to be a poor assumption, because they cannot be determined independently. It was found that both the transition dipole moment and the difference dipole moments of HCN are much larger than they are for the other aliphatic nitriles.

Aromatic Nitriles. With a few exceptions, aromatic nitrile absorption spectra show a single strong band in the nitrile stretch region. A notable exception is the symmetric compound 1,4-dicyanobenzene, which is discussed below with the other symmetric dinitriles. Also, benzonitrile and 2-chloro-benzonitrile show weak absorptions at 16 and 35 cm^{-1} higher frequency, respectively, than the strong nitrile band. The Stark spectra of the small peaks fit well with the same derivative components as the major peaks, but were too small for a thorough analysis. The spectrum of 4-chloro-benzonitrile is shown in Figure 3

TABLE 2: Vibrational Stark Effect Data for Aromatic Nitriles

	absorption data				Stark data					
compound	$\bar{\nu}^a$ cm^{-1}	peak area M^{-1} cm^{-2}	$\|\mathbf{M}\|$ D	q e	A_χ 10^{20} m^2/V^2	B_χ 10^{40} Jm^2/V^2	C_χ 10^{63} J^{2}m^2/V^2	$\|\Delta\boldsymbol{\mu}\|^b$ D/f	$\Delta\alpha_\|^{b,c}$ Å^3/f^2	$A_\|^{b,c}$ Å^3/f
benzonitrile	2227.8	2083	0.093	0.57	2.6	1.52	10.86	0.0361	−0.65	1.00
1,2-dicyanobenzene^d	2235.3	819	0.058	0.36	1.4	2.01	5.80	0.0263	0.60	0.32
1,3-dicyanobenzene^d	2236.3	868	0.060	0.37	5.5	2.23	9.08	0.0330	−0.71	0.92
1,4-dicyanobenzene (A)^{d,e}	2231.7	862	0.060	0.37	2.1	2.76	3.20	0.0196	0.89	0.58
1,4-dicyanobenzene (S)^{d,f}	2243.7	138	0.024	0.15	4.9	1.95	1.30	0.0125	0.43	0.35
2-Cl-benzonitrile	2232.1	1205	0.070	0.43	3.4	1.94	7.81	0.0306	−0.35	0.87
3-Cl-benzonitrile	2232.7	1260	0.072	0.44	2.9	2.04	8.45	0.0318	−0.23	0.82
4-Cl-benzonitrile	2230.6	1921	0.089	0.55	2.7	2.10	10.10	0.0348	−0.26	0.97
4-methoxybenzonitrile	2223.5	3724	0.124	0.76	1.8	1.33	20.60	0.0497	−0.02	0.49

$^{a-c}$ See the corresponding notes in Table 1. ^{d} Peak area and transition dipole are divided by two, to give results on a per nitrile basis. ^{e} Antisymmetric (A) nitrile mode. ^{f} Symmetric (S) nitrile mode.

and its Stark parameters are listed in Table 2 along with those of other aromatic nitriles. As with the aliphatic nitriles, fits to the aromatic Stark spectra are dominated by the second derivative contribution, and the source of the Stark effect is dominated by the difference dipole moment. However, aromatic nitrile VSE spectra exhibit slightly larger zeroth derivative contributions and much larger first derivative contributions, leading to significantly different line shapes. Upon analysis, it is seen that the large first derivative contribution is due to larger difference dipoles and larger transition polarizabilities, rather than to a significant change in difference polarizabilities (Table 2), which are again small and slightly negative. This result contrasts with our earlier work on 4-methoxy-benzonitrile in which it was concluded that the zeroth derivative contribution was sufficiently small to be ignored, and that the entire first derivative contribution represented a positive difference polarizability.[26] The change in interpretation is appropriate, because of the substantial improvement of data quality that has been achieved.

Aromatic nitrile VSE spectra show a relatively large variation in $\|\Delta\boldsymbol{\mu}\|$ values with molecular structure, in contrast to the aliphatic data. As seen in Figure 4, both the transition dipole and difference dipole moments correlate well with Hammett parameters, which are unitless values that characterize the electron donating or electron withdrawing nature of substituents on an aromatic ring.[39] As the transition dipole of a vibrational excitation is directly related to the partial charges on the excited group, the correlation with Hammett parameters is reasonable. The observation that the difference dipoles also correlate with Hammett parameters suggests that $\|\Delta\boldsymbol{\mu}\|$ is determined by the same partial charges, a result which is quantified below and is discussed in a separate publication.[11]

Dinitriles. Centrosymmetric compounds are particularly interesting for Stark analysis because all parameters that are linear with the electric field should vanish by symmetry, including $\Delta\boldsymbol{\mu}$ and **A** (eqs 1 and 2). Also, an inversion symmetric compound has both symmetric and antisymmetric normal modes, where the former are expected to have no absorption intensity and the latter are expected to have twice the intensity observed for comparable nonsymmetric compounds. The symmetric modes would be expected to gain intensity in an electric field due to the symmetry breaking of the field and the effect of the transition hyperpolarizability. Upon a weakening of the coupling between the two nitrile groups of a symmetric compound, relative to coupling to other internal degrees of freedom and to the solvent, the nitrile vibrations become more independent. Thus, absorption and Stark spectra of weakly coupled symmetric dinitriles are expected to approach those of nonsymmetric molecules.
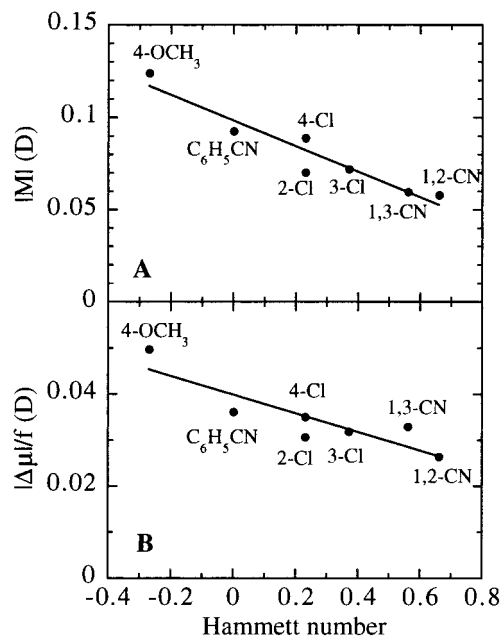

Figure 4. Correlation of the transition dipole and difference dipole moments for the aromatic mononitriles and nonsymmetric aromatic dinitriles with Hammett numbers. 4-OCH$_3$ is 4-methoxybenzonitrile; C$_6$H$_5$CN is benzonitrile; 2-Cl, 3-Cl, and 4-Cl are 2-, 3-, and 4-chlorobenzonitrile; and 1,2-CN and 1,3-CN are 1,2- and 1,3-dicyanobenzene.

As expected, most dinitriles show two absorption peaks in the nitrile stretch region. With the exception of *cis,cis*-mucononitrile (1,4-dicyano-*cis,cis*-1,3-butadiene), one peak is always about an order of magnitude stronger than the other, giving the antisymmetric and symmetric mode assignments, from the discussion above. 1,4-dicyanobenzene (not shown) exhibits strong resonance effects between the two nitrile modes, leading to an absorption spectrum analogous to that of deuterated acetonitrile (Figure 2A, B), and requiring a similar analysis method (eq 9).

The VSE predictions are borne out in the symmetric dinitrile data, presented in Table 3 and Figure 5, although other factors partially obscure this simple picture. In particular, the symmetric and antisymmetric mode frequencies are close enough for dinitriles that there is often significant intensity sharing between the bands due to nonlinear coupling.[36] It is also calculated that approximately 7% of succinonitrile (dicyanoethane) and 12% of adiponitrile (1,4-dicyanobutane) molecules are expected to be in low symmetry conformations.[38] Additionally, the dinitrile Stark data often exhibited a poor signal-to-noise ratio due to low intensity absorptions, small Stark effects, and low dinitrile solubilities in 2-MeTHF. Cyanogen[40] is likely to be an especially

TABLE 3: Vibrational Stark Effect Data for Aliphatic Dinitriles

compound	absorption data				Stark data					
	$\bar{\nu}^a$ cm^{-1}	peak area M^{-1} cm^{-2}	$|\mathbf{M}|$ D	q e	A_χ 10^{20} m^2/V^2	B_χ 10^{40} Jm^2/V^2	C_χ 10^{63} J^{2}m^2/V^2	$|\Delta\boldsymbol{\mu}|^b$ D/f	$\Delta\alpha_{||}^{b,c}$ Å^3/f^2	$A_{||}^{b,c}$ Å^3/f
succinonitrile	2249.9	374	0.039	0.24	4.7	0.04	6.42	0.0277	−1.58	0.57
adiponitrile (A)^e	2244.4	697	0.053	0.33	0	0.70	5.75	0.0262	0.42	0
adiponitrile (S)^f	2261.4	68	0.017	0.10	0	4.74	6.28	0.0274	2.84	0
fumaronitrile (S)^f	2225.0	23	0.010	0.06	192.0	4.87	4.71	0.0237	−5.91	0.91
fumaronitrile (A)^e	2236.5	268	0.033	0.20	0	0.32	0.71	0.0092	0.19	0
1,4-dicyano-2-butene	2251.3	515	0.046	0.28	0.2	1.24	2.84	0.0183	0.62	0.09
cis,cis-mucononitrile (L)^g	2214.7	587	0.049	0.30	9.7	3.15	2.45	0.0171	0.46	1.03
cis,cis-mucononitrile (H)^h	2223.1	548	0.048	0.29	0.9	−0.16	2.38	0.0168	−0.38	0.21

$^{a-c}$ See the corresponding notes in Table 1. ^{d} Peak areas and transition dipoles are divided by two to give results on a per nitrile basis. ^{e} Antisymmetric (A) nitrile mode. ^{f} Symmetric (S) nitrile mode. ^{g} Low (L) energy peak. h) High (H) energy peak.
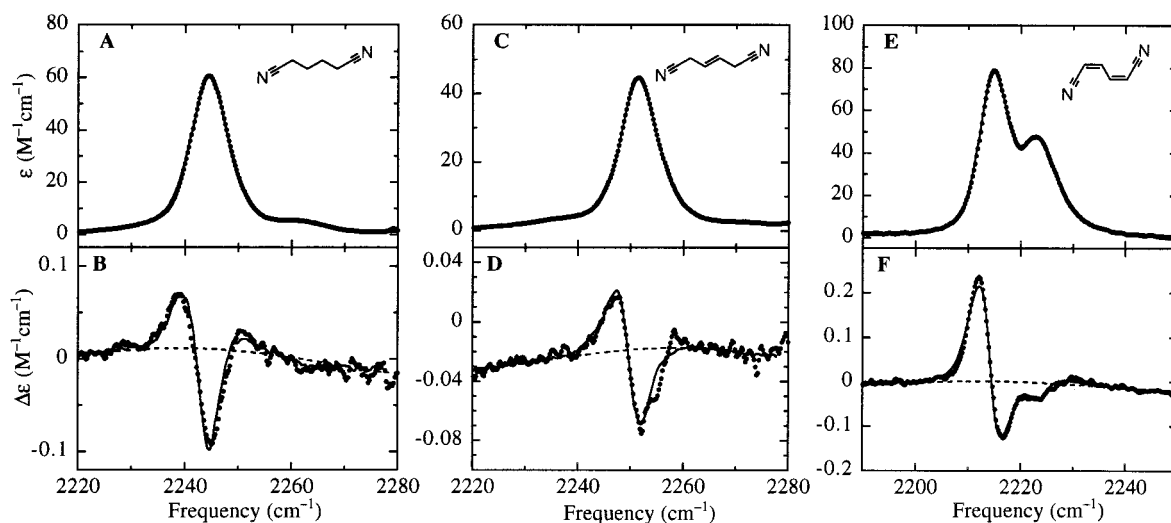
Figure 5. Spectra of a homologous series of dinitriles. (A, B) Extinction coefficient and Stark spectra of adiponitrile (1,4-dicyanobutane); peaks at 2244 and 2261 cm^{-1} represent the antisymmetric and symmetric modes, respectively. The solid line in panel A is a fit of modified Voigts, which was used to separate the measured absorption into two bands. (C, D) Extinction coefficient and Stark spectra of 1,4-dicyano-2-butene. The VSE spectrum is fit with the numerical derivatives of the absorption. (E, F) Extinction coefficient and Stark spectra of *cis,cis*-mucononitrile (1,4-dicyano-*cis,cis*-1,3-butadiene). The VSE spectrum is fit with analytical derivatives of two modified Voigt line shapes, fit to the absorption in panel E.

interesting compound due to its high symmetry and strong internal coupling, but was found to be insoluble in 2-MeTHF and thus could not be analyzed.

Whereas significant linear Stark effects were seen for all dinitriles studied, the difference dipole moments for both bands were invariably lower for dinitriles than for the comparable mononitriles, as expected from the discussion above. Furthermore, the $|\Delta\boldsymbol{\mu}|$ values for both bands decreased with increased conjugation of the hydrocarbon bridge, in agreement with their having greater mechanical coupling between the nitriles. This trend (Figure 5) starts with succinonitrile and adiponitrile (Figure 5A, B), which have $|\Delta\boldsymbol{\mu}|$ values and Stark spectra that are similar to those of aliphatic mononitriles. Increasing the succinionitrile conjugation to give fumaronitrile (dicyanoethene) and the adiponitrile conjugation to give 1,4-dicyano-2-butene (Figure 5C, D) and *cis,cis*-mucononitrile (Figure 5E, F), yield significantly different Stark spectra with progressively smaller second derivative components, implying smaller difference dipoles. The presence of low symmetry conformations may contribute to the observed trend, but this contribution is expected to be small based on the conformational calculations presented above.

Angle Dependence: After a survey of the Stark effects of a diverse collection of nitriles, acetonitrile (Figure 1) and 4-chloro-benzonitrile (Figure 3) were chosen for more detailed analysis due to their single nitrile peaks, minimal resonant interactions, high extinction coefficients, and high molecular symmetry. To examine the one-dimensional assumptions made above, the

zeroth, first, and second derivative fit contributions were plotted as a function of the angle parameter, $1 - 3\cos^2\chi$ (Figure 6). For a purely one-dimensional system ($\zeta = 0°$ and off-diagonal and perpendicular components of $\Delta\boldsymbol{\alpha}$ and $\mathbf{A}$ are zero), the theoretical slope-to-intercept ratio for all three derivative contributions is 0.4, using eqs 4−6.

It was found that 4-chloro-benzonitrile exhibits nearly one-dimensional behavior for all three derivative components, with $\zeta = 5°$, $A_\perp/A_{||} = 0.11$, and $\Delta\alpha_\perp/\Delta\alpha_{||} = -0.001$. Using the fits to the angle dependent data, $|\Delta\boldsymbol{\mu}|$ is 0.0348 D/f, $A_{||}$ is 1.09 Å^3/f, and $\Delta\alpha_{||}$ is -0.20 Å^3/f^2, which are in close agreement with the values calculated with the one-dimensional approximations (Table 2).

Acetonitrile only exhibits one-dimensional behavior for the second derivative component, showing much steeper slopes for the other two components. Analysis shows that $\cos\zeta = 1.04 \pm 0.002$ (clearly leading to an impossible ζ value), $A_\perp/A_{||} = 0.39$, $\Delta\alpha_\perp/\Delta\alpha_{||} = 0.043$, $|\Delta\boldsymbol{\mu}| = 0.0263$ D/f, $A_{||} = 0.79$ Å^3/f, and $\Delta\alpha_{||} = -0.60$ Å^3/f^2. The latter three parameters, $|\Delta\boldsymbol{\mu}|$, $A_{||}$, and $\Delta\alpha_{||}$, are in moderate agreement with the values calculated with the one-dimensional assumptions (Table 1). From the polarizability ratios, $A_\perp/A_{||}$ and $\Delta\alpha_\perp/\Delta\alpha_{||}$, the dominant cause of both the zeroth and first derivative slopes would be interpreted to be a significant transition polarizability perpendicular to the bond axis. However, due to the 3-fold rotational symmetry of acetonitrile, a perpendicular component (or an off-diagonal component) of the transition polarizability cannot occur without significant sym-

Vibrational Stark Effects of Nitriles

*J. Phys. Chem. A, Vol. 104, No. 51, 2000* **11861**
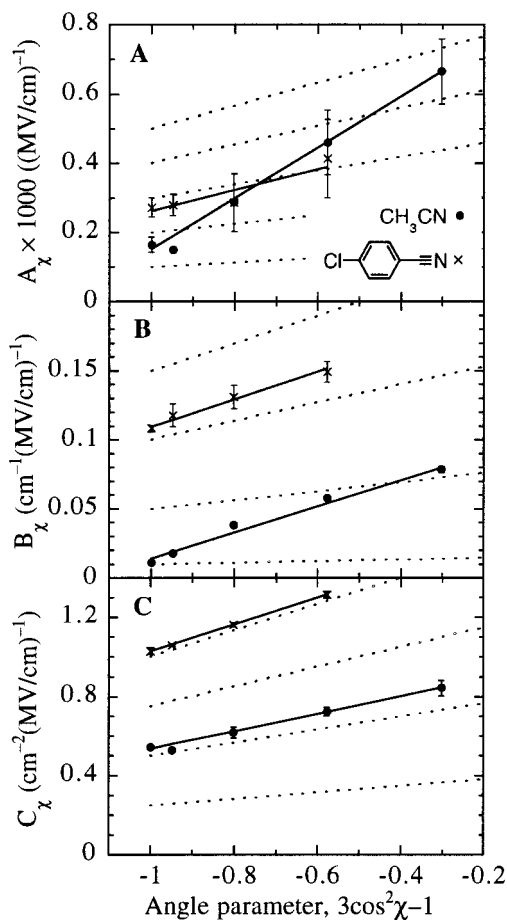
Figure 6. Polarization angle dependence of the fit coefficients for acetonitrile (circles) and 4-chlorobenzonitrile (crosses). Error bars represent one standard deviation. Dashed lines are drawn with a slope-to-intercept ratio of 0.4 as guides to show the expected behavior for fit coefficients of one-dimensional systems (see text).

metry breaking by asymmetric solvation. A more likely explanation is that the band shape of the nitrile mode changes in an electric field, most likely due to the weak Fermi resonant band 50 cm^{-1} to higher energy. This possibility is explicitly ignored in the Stark analysis presented here, likely leading to a mis-interpretation of the A_χ, B_χ, and C_χ angle dependence. This explanation is supported by the observation that statistically significant curvature is seen in Figure 6B for acetonitrile and that $\cos\zeta > 1$, neither of which can be explained by the theory.

Discussion

It is found that difference dipoles correlate well with transition dipoles for all the mononitriles (Figure 7), where the slope of a linear fit is 0.33/f and the intercept is 0.007 D/f. Dinitrile $|\Delta\boldsymbol{\mu}|$ values generally agree with the correlation as well, but with significantly more scatter. In agreement with the predictions above, symmetric dinitriles exhibit small difference dipoles for both symmetric and antisymmetric modes and small transition dipoles for symmetric modes. The decrease of transition dipoles for antisymmetric modes (computed on a per nitrile basis) is expected for electrostatic reasons since two electron withdrawing groups compete for a finite amount of polarizable charge, thus decreasing the amount of partial charge on each nitrogen.

The correlation for mononitriles can be interpreted with a very simple model, which is presented elsewhere in more
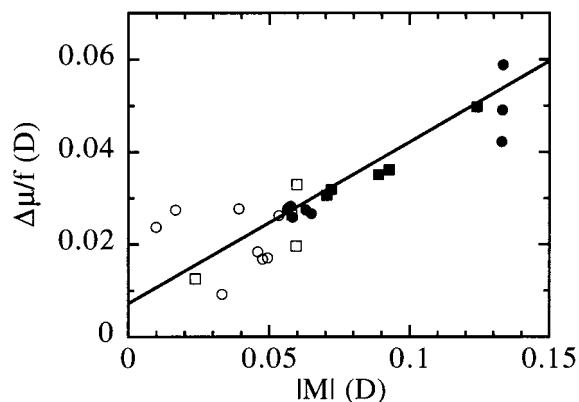
Figure 7. Correlation of difference dipoles with transition dipoles for all samples. Solid circles represent aliphatic mononitriles, solid squares represent aromatic mononitriles, open circles represent aliphatic dinitriles, and open squares represent aromatic dinitriles. The solid line is the best fit to the aliphatic and aromatic mononitrile data, with a slope of 0.33/f and intercept of 0.007 D/f.

detail.[11,22,20] The transition dipole of an harmonic oscillator is given by

$$|\mathbf{M}| = \frac{q}{2\pi}\sqrt{\frac{h}{2cm\bar{\nu}}} \tag{10}$$

where q is the effective charge of the oscillator and m is the reduced mass. From AM1 calculations on the mononitriles studied here, reduced masses are found to be 6.55 ± 0.05 atomic mass units, where the small range reflects the fact that nitrile vibrations are highly localized to the nitrile group. As the vibrational frequency is similar for all the mononitriles as well, the variation of the transition dipoles reflects, for the most part, the variation of the effective charge.

A simple interpretation of the difference dipole is that it reflects a displacement of the effective charge by a distance Δx, where the displacement is due to the anharmonicity of the potential surface

$$|\Delta\boldsymbol{\mu}| = q\Delta x \tag{11}$$

From eqs 10 and 11, the slope of the correlation shown in Figure 7 (with slight corrections to account for the different $\bar{\nu}$ values) corresponds to a Δx value of 0.012 Å/f. The physical interpretation is that the expectation value of the C−N bond length is 0.012 Å/f longer in the first vibrationally excited state than it is in the ground state. This displacement can be compared against that expected from published values of the anharmonicity. In a perturbed harmonic oscillator model,[41] the potential is defined as

$$U(x) = \frac{k}{2}x^2 + \frac{\gamma_3}{6}x^3 \tag{12}$$

The cubic anharmonicity of the C−N bond, γ_3, has been determined from HCN vapor phase spectroscopic data[42] to be 126 aJ/Å^3, leading to a Δx value of 0.0078 Å. Thus, about 70% of the difference dipole values may be explained as being due to nitrile bond anharmonicity (assuming an f value of about 1.1). The discrepancy between the Δx values may result from (*i*) factors other than anharmonicity that contribute to $|\Delta\boldsymbol{\mu}|$ values, (*ii*) differences between the nitrile bond of HCN and of normal modes of larger nitriles, and (*iii*) solvation effects on bond anharmonicity.

In Table 4, hydrogen cyanide and acetonitrile VSE results are compared against theoretical calculations of the molecules

11862 *J. Phys. Chem. A, Vol. 104, No. 51, 2000*

Andrews and Boxer

TABLE 4: Calculated and Observed Vibrational Stark Effects of HCN and CH$_3$CN.

property	unit	HCN obs[a]	HCN calc[b]	CH$_3$CN obs[c]	CH$_3$CN calc[b]
$|\mathbf{M}|$	D	0.134	0.0055	0.0582	0.0172
$|\Delta\boldsymbol{\mu}|$	D	0.05/f	0.0010	0.0263/f	0.0066
$\Delta\alpha_{\|}$	Å^3	$-2/f^2$	0.0402	$-0.60/f^2$	0.0425
$A_{\|}$	Å^3	1.2/f	0.157	0.79/f	0.171
$|\Delta\boldsymbol{\mu}|/|\mathbf{M}|$	unitless	0.37/f	0.182	0.452/f	0.384
$\Delta\alpha_{\|}/|\mathbf{M}|$	(MV/cm)$^{-1}$	$-0.05/f^2$	0.0244	$-0.034/f^2$	0.0082
$A_{\|}/|\mathbf{M}|$	(MV/cm)$^{-1}$	0.03/f	0.0952	0.045/f	0.033

[a] Unweighted averages of the values for the three subbands; assumes one-dimensional behavior and that $\mathbf{B}$ is 0. [b] Highest level of calculation from Reimers and Hush.[22] [c] From data where χ angle dependence was measured; values do not assume one-dimensional behavior, but do assume $\mathbf{B}$ is 0.

in the absence of solvent.[22] It is seen that all of the experimental Stark parameters are several times greater than the calculated values, and are often larger by more than an order of magnitude. However, consideration of the Stark parameters in relation to the transition dipole values results in significantly better agreement. In particular, calculations for the acetonitrile transition polarizability and the difference dipole moment are within about 25% of the measured values. The large discrepancies seen for hydrogen cyanide are not surprising due to the strong solvent effects that were observed.

Conclusions

A method for measuring vibrational Stark spectra has been developed and applied to the infrared absorption of the nitrile stretch mode of several aliphatic and aromatic nitriles. While most compounds were not analyzed enough times for detailed error estimates, the precision of the method can be reasonably estimated by averaging the standard deviations for all repeated experiments. Difference dipoles, which invariably dominated the Stark effects, were reproducible to within ±0.001 D/f, giving a Stark tuning precision of $\pm0.02/f$ cm^{-1}/(MV/cm). Difference polarizabilities and transition polarizabilities led to smaller absorption changes, and could be measured reliably with precisions of 0.3 Å^3/f^2 and 0.1 Å^3/f, respectively.

The VSE data show that $|\Delta\boldsymbol{\mu}|$ values are typically smallest for symmetric dinitriles, larger for aliphatic nitriles and largest for aromatic species. The values of $|\Delta\boldsymbol{\mu}|$ are virtually all within the range of 0.01 D/f to 0.04 D/f, which is several orders of magnitude smaller than typical values for electronic Stark effects[24] and a factor of 2 to 8 smaller than those seen for the VSE of carbon monoxide[1] or nitric oxide[2] bound to the heme iron in myoglobin and heme model compounds. Where comparable experimental data exist, the $|\Delta\boldsymbol{\mu}|$ values are in good agreement.[26,9] Compared to theoretical results, they are several times larger than those predicted from *ab initio* calculations for isolated molecules,[22] but agreement improves significantly when Stark parameters are considered relative to transition dipoles.

While the nitrile stretch mode is typically well separated from other molecular vibrations, only about half of the samples studied exhibited well defined single bands. The other samples had multiple bands arising from Fermi resonant interactions, varying degrees of hydrogen bonding, and perhaps multiple sample conformations. Most dinitriles exhibited multiple bands as well, reflecting symmetric and antisymmetric stretch modes. It was found that Stark parameters were generally similar for bands that arose from Fermi resonance, whereas they differed between bands arising from different modes. While the dinitrile data were not as simple as their symmetry might suggest, both

Stark and absorption results agreed with expected trends, showing small difference dipoles and greater symmetry effects upon improved mechanical coupling.

For the aromatic nitriles studied, Hammett numbers correlate with both transition dipole moments and $|\Delta\boldsymbol{\mu}|$ values, likely making them a good predictive tool. More broadly, it was shown that transition dipoles correlate well with $|\Delta\boldsymbol{\mu}|$ values for all mononitriles and, to a lesser extent, for dinitriles. To a large extent, the correlation for mononitriles is consistent with that expected from the anharmonicity of the nitrile bond. However, Stark effects are larger than just those expected from anharmonicity, suggesting that other contributions are important as well.

The ability to routinely measure vibrational Stark effects to good precision makes it possible to investigate molecular vibrations in condensed phases in a new and sensitive manner. This technique has previously been shown to be useful for measuring an electric field change in a series of myoglobin mutants,[1] and has been studied here to clarify the physical origins of vibrational Stark effects.

References and Notes

(1) Park, E. S.; Andrews, S. S.; Hu, R. B.; Boxer, S. G. *J. Phys. Chem. B* **1999**, *103*, 9813.
(2) Park, E. S.; Thomas, M. R.; Boxer, S. G. *J. Am. Chem. Soc.*, in press.
(3) Onsager, L. *J. Am. Chem. Soc.* **1936**, *58*, 1486.
(4) Stryer, L. *Biochemistry*, Fourth ed.; W. H. Freeman and Company: New York, 1995.
(5) Laberge, M.; Sharp, K. A.; Vanderkooi, J. M. *J. Phys. Chem. B* **1997**, *101*, 7364.
(6) Phillips, G. N. J.; Teodoro, M.; Li, T.; Smith, B.; Gilson, M. M.; Olson, J. S. *J. Phys. Chem. B* **1999**, *103*, 8817.
(7) Kolling, O. W. *J. Phys. Chem.* **1996**, *100*, 16087.
(8) Nyquist, R. A. *App. Spectrosc.* **1990**, *44*, 1405.
(9) Spitzer, R. C.; Sievers, A. J.; Silsbee, R. H. *J. Opt. Soc. Am. B* **1992**, *9*, 978.
(10) Lambert, D. K. *J. Chem. Phys.* **1988**, *89*, 3847.
(11) Andrews, S. S.; Boxer, S. G., in preparation.
(12) AM1 level calculations using MacSpartan (Wave function Inc.).
(13) Charles, S. W.; Cullen, F. C.; Owen, N. L. *J. Mol. Struct.* **1976**, *34*, 219.
(14) DeLeon, R. L.; Muenter, J. S. *J. Chem. Phys.* **1984**, *80*, 3992.
(15) Kumar, A. P.; Rao, G. R. *Sepctrochim. Acta Part A* **1997**, *53*, 2033.
(16) Michel, H.; Lippert, E. Acetonitrile-The structure of the liquid and solid phases and the nature of the liquid−solid-phase transition. In *Organic Liquids. Structure, dynamics, and chemical properties*; Buckingham, A. D., Lippert, E., Bratos, S., Eds.; John Wiley & Sons: New York, 1978; p 293.
(17) Pace, E. L.; Noe, L. J. *J. Chem. Phys.* **1968**, *49*, 5317.
(18) Reimers, J. R.; Hall, L. E. *J. Am. Chem. Soc.* **1999**, *121*, 3730.
(19) Thomas, B. H.; Orville-Thomas, W. J. *J. Mol. Struct.* **1971**, *7*, 123.
(20) Hush, N. S.; Reimers, J. R. *J. Phys. Chem.* **1995**, *99*, 15798.
(21) Mathies, R. A. Experimental and theoretical studies on the excited electronic states of some aromatic hydrocarbons through electric field perturbation and through chemical substituents, Cornell University, 1974.
(22) Reimers, J. R.; Zeng, J.; Hush, N. S. *J. Phys. Chem.* **1996**, *100*, 1498.
(23) Wortmann, R.; Bishop, D. M. *J. Chem. Phys.* **1998**, *108*, 1001.
(24) Bublitz, G. U.; Boxer, S. G. *Annu. Rev. Phys. Chem.* **1997**, *48*, 213.
(25) Jucks, K. W.; Miller, R. E. *J. Chem. Phys.* **1988**, *88*, 6059.
(26) Chattopadhyay, A.; Boxer, S. G. *J. Am. Chem. Soc.* **1995**, *117*, 1449.
(27) Andrews, S. S.; Boxer, S. G. *Rev. Sci. Inst.* **2000**, *71*, 3567.
(28) Long, F.; Freedman, T. B.; Tague, T. J.; Nafie, L. A. *Appl. Spectrosc.* **1997**, *51*, 508.

Vibrational Stark Effects of Nitriles

J. Phys. Chem. A, Vol. 104, No. 51, 2000 **11863**

(29) Three factors appear to improve the signal-to-noise for rapid-scan methods relative to step-scan methods: (*i*) it is not necessary to wait for a lock-in to settle after each mirror step, (*ii*) multiplexing of signal frequencies is used, and (*iii*) interferogram oversampling requires no additional time. This is discussed more fully in Andrews, S. S.; Boxer, S. G. In preparation.

(30) Early experiments were performed in a miniature Joule-Thompson refrigerator (MMR Technologies) operating at 80 K, but we found significant sample orientation in an electric field, leading to the development of the immersion cryostat. Poling may not be a problem for AC electric fields.

(31) Data fitting was done with Macintosh software created for this purpose. The software and C language source code are available upon request.

(32) The parameters of a modified Voigt are: peak height, frequency, full width at half-maximum, and the Gaussian:Lorentzian ratio. These parameters are adjusted only to obtain a best fit to the absorption spectrum, and are not considered to have any physical meaning.

(33) Assuming the maximum possible ζ angle of 90° and the maximum sample rotation angle of $\chi = 20°$, C_χ would be corrected to be 13% too small under the one-dimensional assumptions, contributing to a 7% error in the calculation of $|\Delta\boldsymbol{\mu}|$.

(34) Atkins, P. W. *Physical Chemistry*, 5th ed.; W. H. Freeman and Company: New York, 1994.

(35) Smith, A. L.; Keller, W. E.; Johnston, H. L. *Phys. Rev.* **1950**, *79*, 728.

(36) Linear coupling between two modes results in redefined normal modes and a separation of the absorption peaks, whereas nonlinear coupling gives absorption between the peaks, and is responsible for Fermi resonance. The excess absorption is analogous to the coalescence seen in NMR spectra of dynamic systems (see e.g. Gasparro, F. P.; Kolodny, N. H. *J. Chem. Educ.* **1977**, *54*, 258−261).

(37) Miller, T. M. Atomic and molecular polarizabilities. In *Handbook of Chemistry and Physics*, 71st ed.; Lide, D. R., Ed.; CRC Press: Boca Raton, FL, 1990; p 10.

(38) The transition state enthalpy is expected to be about 16 kJ/mol, from butane data (see e.g., Kemp, D. S.; Vellaccio, F. *Organic Chemistry*; Worth Publishers: New York, 1980; p. 472), implying an interconversion rate below 1 ms down to the 100 K glass transition temperature, which is fast compared to the freezing rate. Thus, low-temperature population ratios were computed for 100 K, with the assumption that the sample is at equilibrium before freezing and immobilized thereafter. Boltzmann population calculations use an enthalpy difference between *anti* and *gauche* conformations of 2.8 kJ/mol, a value found by AM1 calculations for the relevent nitriles.

(39) Lowry, T. H.; Richardson, K. S. *Mechanism and Theory in Organic Chemistry*, 3rd ed.; Harper Collins: New York, 1987.

(40) Cyanogen was synthesized by an adaptation of a method from: Janz, George J. *Inorg. Synth.* **1957**, 5, 43−48.

(41) McQuarrie, D. A. *Quantum Chemistry*; University Science Books: Sausalito, CA, 1983.

(42) Strey, G.; Mills, I. M. *Mol. Phys.* **1973**, *26*, 129.